# On the illumination invariance of the level lines under directed light. Application to change detection.

Pierre Weiss, Alexandre Fournier, Laure Blanc-Féraud, Gilles Aubert

INSTITUT NATIONAL DE RECHERCHE EN INFORMATIQUE ET EN AUTOMATIQUE

# *On the illumination invariance of the level lines under directed light Application to change detection*

Pierre Weiss — Alexandre Fournier — Laure Blanc-Féraud — Gilles Aubert

**N° 6612**

August 2008

Thème COG


ISSN 0249-6399 ISRN INRIA/RR--6612--FR+ENG

# On the illumination invariance of the level lines under directed light
# Application to change detection

Pierre Weiss , Alexandre Fournier , Laure Blanc-Féraud , Gilles Aubert

Thème COG — Systèmes cognitifs
Projets Ariana

Rapport de recherche n° 6612 — August 2008 — 33 pages

**Abstract:** We analyze the illumination invariance of the level lines of an image. We show that if the scene surface has Lambertian reflectance and the light is directed, then a necessary condition for the level lines to be illumination invariant is that the 3D scene be developable and that its albedo satisfies some geometrical constraints. We then show that the level lines are "almost" invariant for piecewise developable surfaces. Such surfaces fit most of the urban structures. In a second part, this allows us to devise a very fast algorithm that detects changes between pairs of remotely sensed images of urban areas, independently of the lighting conditions. We show the effectiveness of the algorithm both on synthetic OpenGL scenes and real Quickbird images. We compare the efficiency of the proposed algorithm with other classical approaches and show that it is superior both in practice and in theory.

**Key-words:** Level lines, topographic map, illumination invariance, contrast equalization, change detection, remote sensing

Unité de recherche INRIA Sophia Antipolis
2004, route des Lucioles, BP 93, 06902 Sophia Antipolis Cedex (France)
Téléphone : +33 4 92 38 77 77 — Télécopie : +33 4 92 38 77 65

# Sur l'invariance aux changements d'illumination des lignes de niveau. Application à la détection de changements.

**Résumé :** Nous analysons l'invariance aux changements d'illumination des lignes de niveau d'une image. Nous montrons que si la surface de la scène est lambertienne et que la lumière est direcrtionnelle, alors une condition nécessaire et suffisante pour que les lignes de niveau soient invariantes est que la scène 3-D sous-jacente soit développable et que son albédo varie seulement dans certaines directions de l'espace. Nous montrons ensuite la quasi-invariance des lignes de niveau pour des surface développable par morceaux. De telles surface modélisent bien la plupart des structures urbaines. Dans une deuxième partie, nous utilisons ce résultat pour contruire un algorithme de détection de changements sur des paires d'images satellitaires. Cet algorithme est très rapide et fonctionne indépendamment des conditions d'illuminations. Nous montrons l'efficacité de cette approche à la fois sur des images de synthèse OpenGL et sur des images réelles de télédétection. Nous comparons l'efficacité de cet algorithme avec d'autres approches classiques et nous montrons sa supériorité théorique et pratique.

**Mots-clés :** norme $l^\infty$, minimisation de la variation totale, bruits bornés, bruits de compression, bruits de quantification, dualité, descente de sous-gradient projeté

# Contents

# 1 Introduction

Finding illumination invariant features in an image is a recurrent problem in computer vision (see for instance [7, 28] and the references therein). There are many important applications that would benefit from such features including recognition, contrast equalization/enhancement, image registration and change detection.

Perhaps the most frequently used feature is the set of contours [24]. Contours are generally due to discontinuities in the scene elevation or albedo and are illumination invariant in the sense that they appear on an image for most lighting conditions. An alternative feature was recently proposed by V. Caselles et al. [3]. The authors show that the *level lines* are invariant to *local contrast changes*. The set of all level lines (also called topographic map) has two important advantages over the contours. First, in the discrete setting, the definition of a contour generally depends upon a thresholding parameter while the topographic map does not. Second, the topographic map allows to reconstruct an image. Some applications of the topographic maps - like change detection [27, 1], registration [26] or contrast enhancement [5] - were recently proposed and lead to good results. However local contrast changes [3] cannot model all *illumination changes* (i.e. variations of the illumination conditions). Figure (1) gives an example of a surface the level lines of which are not illumination invariant. Those methods are thus not fully justified.

In this work, we provide necessary conditions on the scene geometry, for the level lines to be invariant to variations of the incident light direction. In the first part of this paper, we show that they are invariant only if the scene surface is developable and that its albedo varies in only certain directions of the space. Such surfaces are of little interest as they are not met in real scenes. This leads us to analyse the level line invariance for piecewise developable surfaces. We show that the images of such objects have "almost" invariant level lines. While writing this paper we discovered a work by H. Chen et al. [7] which shows that the direction of the gradient is "almost" invariant to the light direction of incidence for most scenes. To our knowledge, this result is the closest to our conclusions.

In the second part we use the level lines to devise an algorithm adapted to the detection of changes between pairs of registered images. Many man-made structures can be considered piecewise developable. This algorithm is thus particularly adapted to the detection of changes between image pairs of civil infrastructures or high resolution images of urban areas. We focus on the second application. Previous authors had already tried to design change detection algorithms robust to illumination changes. The surveys on change detection by Radke et al. [30] and Lu et al. [22] give some examples of such algorithms. Early attempts include linear contrast equalization [40], local mean and variance normalizations [18], use of the ratio image [36, 38] or global contrast enhancement [35]. Such approaches have a main weakness: they do not reproduce all the possible illumination changes. Our experiments using them led to large amounts of false positives. Two works are more closely related to our approach. In [38], the authors make the assumption that the building roofs are flat and have Lambertian reflectance. Under these assumptions, they show that the ratio image can be used to detect shadows and changes independently of the light direction. Their hypotheses on the scene are however much more restrictive than ours. In [27, 1], the authors propose

an interesting change detection algorithm that makes large use of the level lines. However, we will show both theoretically and experimentally that their definition of the level lines do not make them illumination invariant features.

Finally we compare different approaches on synthetic images and high resolution Quickbird images. This analysis gives a clear advantage to our method. Let us point out that there exist many other algorithms based on other invariant features. For instance, [34] uses features like the Harris corner detector, while [23] evaluates a non-local illumination rescaling. Those methods are however difficult to compare with our approach since they require many decision steps and many implicit parameters.

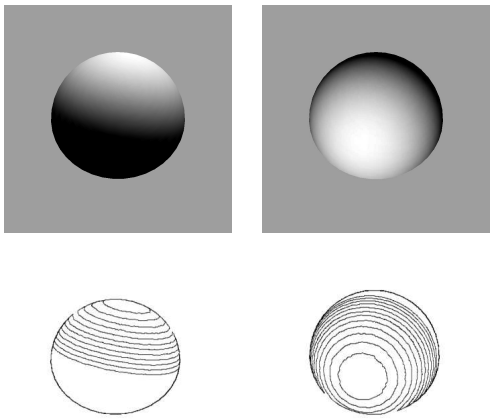

Figure 1: Top: images of a 3-D dome illuminated with Phong model [29] using two different incident light directions. Bottom: some of their level lines.

# 2 Notations, hypotheses, definitions

## 2.1 Notations

Let $\Omega$ be an open connected set of $\mathbb{R}^2$. Let $u : \Omega \to \mathbb{R}$ be some $C^2$ function. $\nabla u = [u_1, u_2]$ denotes the gradient of $u$, $\nabla^2 u = \begin{bmatrix} u_{11} & u_{12} \\ u_{12} & u_{22} \end{bmatrix}$ denotes its Hessian matrix. Let $p : \mathbb{R}^2 \to \mathbb{R}^2$, $J(p)$ denotes the Jacobian of $p$. Let $x$ and $y$ belong to $\mathbb{R}^n$. $x \,/\!/\, y$ means that $x$ and $y$ are colinear. 0 is colinear to any element of $\mathbb{R}^n$. Let $\omega \subset \Omega$, $\overline{\omega}$ is the closure of $\omega$ (w.r.t. the topology induced by the Euclidean metric). $\mathring{\omega}$ and $\text{int}(\omega)$ denote the interior of $\omega$ defined as the largest open set contained in $\omega$. $\mu_{\mathbb{R}^n}$ is the Lebesgue measure on $\mathbb{R}^n$. $\mathcal{M}_{m,n}$ is the space of matrices with $m$ rows and $n$ columns.

The following notations are illustrated in Figure 2. $\Omega$ represents the image plane. It is an open connected set of $\mathbb{R}^2$. $\mathbf{\Omega}$ represents the object plane. $s : \mathbf{\Omega} \to \mathbb{R}$ designates the scene elevation. $N(\mathbf{x})$ represents the normal to the scene surface at point $(\mathbf{x}, s(\mathbf{x}))$. $P : (\mathbf{x}, z) \mapsto x$ is a perspective projection on $\Omega$. $p$ is the application defined by:

$$\begin{array}{rccc} p: & \mathbf{\Omega} & \to & \Omega \\ & \mathbf{x} & \mapsto & P(\mathbf{x}, s(\mathbf{x})) \end{array} \tag{1}$$

We suppose that $p$ is a $C^1$ diffeomorphism. As a diffeomorphism is bijective, it means physically that the camera can see all points of the surface.

Throughout the article, bold fonts refer to objects that lie in the object plane, while type fonts stick to objects in the image plane. For instance $\mathbf{\Omega} = p^{-1}(\Omega)$ represent the object plane. If $x \in \Omega$, we can define $\mathbf{x} = p^{-1}(x)$ which is a point of $\mathbf{\Omega}$.

Finally, $l$ is a vector in $\mathbb{R}^3 \backslash \{0\}$. $\frac{l}{|l|}$ denotes the light incidence direction and $|l|$ denotes its intensity.

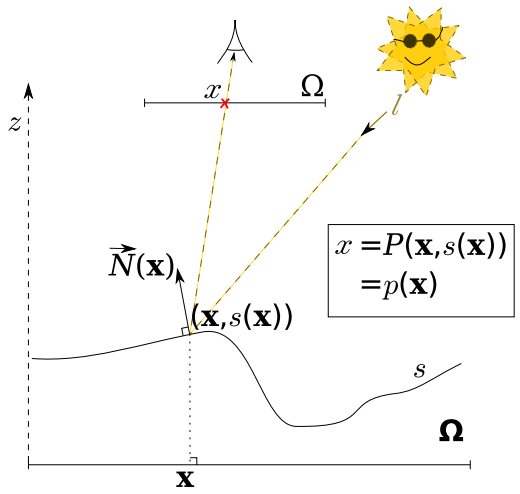


Figure 2: Notations

## 2.2 Hypotheses on the surface and the light

To model the interactions between a surface and the light, we use Phong reflectance model [29]. We make the following hypotheses on the light and the surface:

**Hypothesis 1.** *We consider that the light is composed of ambient light of amplitude $\gamma$ (light present everywhere uniformly in the scene) and directed light $l$ (all light rays are parallel with equal intensity).*

**Hypothesis 2.** *We suppose that the surface is Lambertian with variable albedo* $\alpha : \mathbb{R}^2 \to \mathbb{R}_*^+$ *[12].*

**Hypothesis 3.** *To avoid the presence of shadows we suppose that the angle between* $l$ *and* $N$ *is strictly less than* $\pi/2$ *in a non-empty open set* $\mathcal{L} \subset \mathbb{R}^3$*. The set of all possible lighting conditions* $[l, \gamma]$ *is denoted* $\mathscr{L} = \mathcal{L} \times \mathbb{R}^+$*.*

With these hypotheses a scene $S$ is completely described by $S = (s, \alpha)$ and the lighting conditions are completely described by the vector $L = [l, \gamma] \in \mathscr{L}$. Under the Lambertian assumption, the image $u$ of the scene $S$ under lighting conditions $L$ can be written as [29]:

$$u_{S,L}(x) = (\langle l, N(\mathbf{x})\rangle + \gamma) \cdot \alpha(\mathbf{x}) \tag{2}$$

where $\langle \cdot, \cdot \rangle$ stands for the canonical scalar product.

**Note:** All the results stated later are also valid for the following model of image formation:

$$u_{S,L}(\mathbf{x}) = \phi\left((\langle l, N(\mathbf{x})\rangle + \gamma) \cdot \alpha(\mathbf{x})\right) \tag{3}$$

where $\phi : \mathbb{R} \to \mathbb{R}$ is a strictly monotonic function modeling a global contrast change. To simplify the notations, we only make use of model (2).

## 2.3 Definitions of the level lines

Let $u : \Omega \to \mathbb{R}$ be some function. We suppose that $u$ is defined everywhere. Throughout the paper the term level line must be understood in the following way:

**Definition 1** (Level lines)**.** *The level lines of* $u$ *are the connected components [14] of the isolevels* $\{x \in \Omega, u(x) = \lambda\}$*.*

This definition is generally used for $C^1$ functions with non vanishing gradient. For such functions, the level lines can be shown to be Jordan curves that are either closed or the extremities of which lie on the boundary of $\Omega$. For other functions the level lines can be any connected object of the plane like points, curves, planes, fractals... The term "line" is thus a misuse of language. In [3, 11], the authors gave a different definition of the level lines:

**Definition 2** (Level lines [3, 11])**.** *Let* $u$ *be an upper semi-continuous function. The level lines of* $u$ *are defined as the boundaries of the connected components of the level sets* $\{x \in \Omega, u(x) \leq \lambda\}$*.*

Level lines thus defined are curves. However, we will show that they are not illumination invariant even for very simple scenes.

# 3 Level line invariance

In this part we characterize the scenes that produce illumination invariant level lines. All the proofs of the following results are in the appendix. We first suppose that $s$ is $C^2$ and $\alpha$ is $C^1$. This implies that $u_{S,L}$ is $C^1$ for any $L \in \mathscr{L}$. Let us recall two important definitions of differential geometry:

**Definition 3** (Gaussian curvature)**.** *The Gaussian curvature of a surface in* $\mathbb{R}^3$ *is defined as the product of its two principal curvatures. With our notations, the Gaussian curvature of* $s$ *is defined as* $\det(\nabla^2 s)$.

**Definition 4** (Developable surface)**.** *A* $C^2$ *surface which has a zero Gaussian curvature on every point is called developable [32]. Simple examples of such objects are planes, cylinders and cones. A developable surface has the following properties [32]:*

- *Each point of the surface lies on a line (the generatrix) that belongs to the surface.*
- *The plane tangent to the surface is the same on each point of the generatrix.*

Given the two previous definitions, we are now able to introduce the set of scenes which will be proven to generate images with illumination invariant level lines:

**Definition 5.** $\Theta$ *denotes the set of scenes* $S = (s, \alpha)$ *such that* $s$ *is* $C^2$ *developable,* $\alpha$ *is* $C^1$ *and varies only in the direction orthogonal to the generatrices of* $s$*. On points where the scene surface is planar (*$\nabla^2 s = 0$*),* $\alpha$ *can vary in any direction.*

We prove the illumination invariance of the level lines step by step. We first focus on local properties of the images, namely the direction of their gradient. Many contrast invariant algorithms rely on that feature. For instance, the authors of [20] use it for change detection, the authors of [2, 7, 6] use it to compute dissimilarity measures between two images and [9] use it for image registration. The following theorem characterizes the scenes for which those algorithms are fully justified:

**Theorem 1.** *Let* $s \in C^2(\Omega)$ *and* $\alpha \in C^1(\Omega)$*. The following propositions are equivalent:*

- *Prop. 1:* $\forall (L_1, L_2) \in \mathscr{L} \times \mathscr{L},\ \forall x \in \Omega,\ \nabla u_{S,L_1}(x) \mathbin{/\!\!/} \nabla u_{S,L_2}(x)$
- *Prop. 2:* $S \in \Theta$

This means that the direction of the gradient is an illumination invariant feature if and only if the scene belongs to $\Theta$. Let us mention that a recent result of the same kind was obtained in [7, 6]. The authors show that the direction of the gradient is almost illumination invariant in the sense that its distribution w.r.t. the light orientation is concentrated along a given vector for most scenes.

Now let us focus on the results concerning the level line invariance. The previous result allows to easily show the following proposition:

**Corollary 1.** *The level lines are illumination invariant only if the scene belongs to* $\Theta$.

However, all the scenes belonging to $\Theta$ do not have illumination invariant level lines. For instance, Figure (3) shows a cone with constant albedo. If the directed light comes exactly in the direction of the cone axis (left part), the cone radiometry is uniform and the image of the cone is composed of only one level line. In general (right part) the level lines correspond to the cone generatrices.

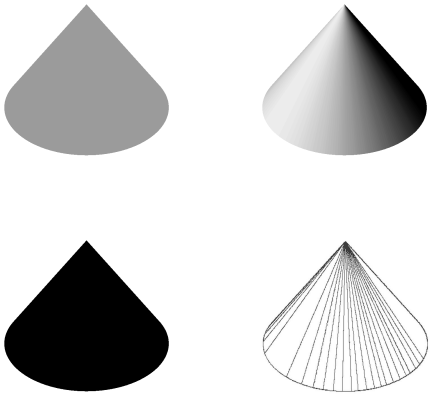

Figure 3: Top: images of a cone illuminated using two different incident light directions. Bottom: some of their level lines.

We can state a weaker result that completes corollary (1):

**Theorem 2.** *Let* $S \in \Theta$. *For almost all pairs of lighting conditions* $(L_1, L_2) \in \mathscr{L} \times \mathscr{L}$ *(w.r.t. the Lebesgue measure of* $\mathbb{R}^4 \times \mathbb{R}^4$*) the level lines of* $u_{S,L_1}$ *are the same as those of* $u_{S,L_2}$.

This theorem and corollary (1) show that there is "almost" an equivalence between the two propositions:

- The scene has invariant level lines.
- The scene belongs to $\Theta$.

Unfortunately, the space $\Theta$ contains too few surfaces to model any real-life scene [1]. This leads us to analyze the level line invariance when $S$ is a piecewise developable $C^2$ mapping

[1] with an exception for warped documents. A warped sheet of paper is developable. This is an alternative definition of the developable surfaces. Theorem (2) could thus be used for the task of document unwarping, independently of the lighting conditions. This remark was already used by some authors [8, 33, 37]

and that its albedo varies orthogonally to the generatrices on each piece. Let us give a precise definition of this space:

**Definition 6** ($\Xi$)**.** *$\Xi$ is the space of scenes $\overline{S} = (\overline{s}, \overline{\alpha})$ such that there exists a finite set $\{\boldsymbol{\omega}_i\}_{i\in I}$ and a scene $S = (s, \alpha)$ which satisfy:*

- *$\forall i \in I$, $\boldsymbol{\omega}_i \subset \boldsymbol{\Omega}$ is an open, connected set of non zero measure.*
- *$\forall (i, j)$, $\boldsymbol{\omega}_i \cap \boldsymbol{\omega}_j = \emptyset$.*
- *$\cup_{i\in I} \overline{\boldsymbol{\omega}}_i = \boldsymbol{\Omega}$.*
- *$\forall i$, $S|_{\boldsymbol{\omega}_i} \in \Theta$ (the restriction of $S$ to $\boldsymbol{\omega}_i$ belongs to $\Theta$).*
- *Finally, we suppose that $S|_{\boldsymbol{\omega}_i}$ (as well as $N|_{\boldsymbol{\omega}_i}$) admits a limit on the boundary of $\boldsymbol{\omega}_i$. This allows to define $\overline{S} = (\overline{s}, \overline{\alpha})$ everywhere. For instance we can define it this way:*

$$\begin{cases} (\overline{s}, \overline{\alpha})(\mathbf{x}) = (s, \alpha)(\mathbf{x}) & \text{if } \mathbf{x} \in \cup_{i\in I} \boldsymbol{\omega}_i \\ \begin{cases} \overline{s}(\mathbf{x}) = \lim\limits_{r\to 0} \sup\limits_{\mathbf{y}\in B(\mathbf{x},r)} s(\mathbf{y}) \\ \overline{\alpha}(\mathbf{x}) = \lim\limits_{r\to 0} \sup\limits_{\mathbf{y}\in B(\mathbf{x},r)} \alpha(\mathbf{y}) \end{cases} & \text{otherwise} \end{cases}$$

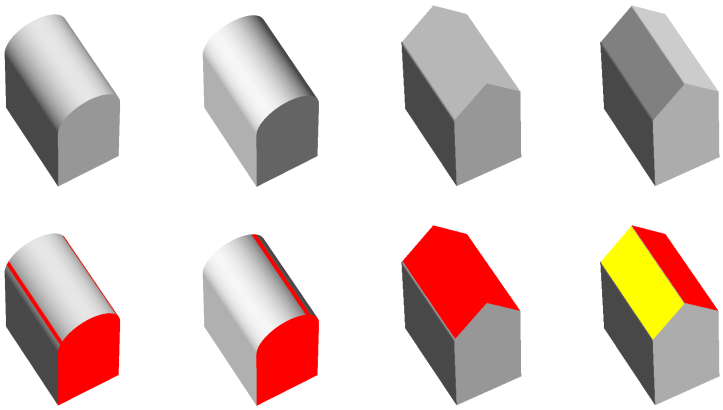

Figure 4: Examples of non invariance of the level lines in the non-smooth case. The colored parts represent singular level lines.

For images generated from scenes in $\Xi$, the level lines have weaker invariance properties than previously. Figures (4) illustrate this fact. On the left part, most of the level lines of the cylinder-shaped roof are just segments on the roof. Depending on the light orientation,

one or two of these segments can merge with the "building wall". Consequently, the level lines are non invariant. Right part of Figure (4) shows the image of a triangle-shaped roof under two different illuminations. This roof is composed of two plane portions. If the light direction belongs to the plane bisecting these portions, then they will have the same radiosity. For most light orientations, the roof will thus be constituted of two level lines (yellow and red), while for a set of zero measure, it can be constituted of only one level set (red). In the following we state those observations in a formal way.

Let $\boldsymbol{\omega}$ be a subset of $\boldsymbol{\Omega}$, and $\mathbf{x} \in \boldsymbol{\Omega}$. We define the following notations:

- $\kappa(\mathbf{x}, L)$ is the level line of $u_{S,L}$ such that $x = p(\mathbf{x}) \in \kappa(\mathbf{x}, L)$;
- $\kappa_\omega(\mathbf{x}, L)$ is the level line of $u_{S,L}|_\omega$, such that $x \in \kappa_\omega(\mathbf{x}, L)$.

**Proposition 1.** *Let $S$ belong to $\Xi$. Let $\omega_i$ and $\omega_j$ be adjacent pieces. Two adjacent level-lines of $u_{S,L}|_{\omega_i}$ and $u_{S,L}|_{\omega_j}$ merge for almost no $L$.*

This proposition can be used to show that the level lines are "almost" invariant in an interesting particular case:

**Corollary 2.** *Let $S$ be a piecewise planar surface with constant albedo on each piece. The level lines of $u_{S,L}$ are the same for almost every $L$.*

This result concludes the theoretical part of this paper.

# 4 An illumination invariant algorithm for change detection

With the previous results in mind, we turn to the problem of change detection. The detection of changes between two grayscale images is a very challenging problem. Some recent theoretical results show that it is in some sense unsolvable. It is indeed impossible (under the Lambertian assumption) to decide whether two images represent the same object or different objects under different illuminations [7]. In practice - to our knowledge - no algorithm is yet able to treat large remotely sensed images of urban areas with a reasonable number of false positives. The main difficulties that arise to design such an algorithm are the changes in illumination, the profusion of details in high resolution images, the parallax errors (see Fig. (5)), and a large number of minor changes that should not be detected. All those difficulties led some authors to let aside the interest of the details provided by high resolution images and to concentrate only on major changes of the urban landscape [20].

However, humans are able to perform change detection manually (though some situations are ambiguous) at the cost of a large amount of time. It thus seems possible to achieve - or at least assist - this task by automatic algorithms. Humans often require some semantic interpretation of the scene to detect changes. It is thus necessary to introduce some priors about the scene geometry. For instance some authors try to find objects the boundaries of

which are lines or polygons [19, 17, 10] as they are likely to be buildings. Other authors assume that the scene elevation is piecewise constant [38]. In this work, we make the assumption that the scene belongs to $\Xi$. We propose a simple algorithm that equalizes the contrast of two images. After this pre-processing step, a simple per-pixel difference gives encouraging results both on synthetic OPENGL images and real Quickbird images.

## 4.1 Underlying hypotheses

Let us recall and justify the assumptions we make on the scenes:

**Hyp.1** the surfaces have Lambertian reflectance.

**Hyp.2** the lighting is a mixture of ambient light and directional light.

**Hyp.3** the scene belongs to $\Xi$.

**Hyp.4** the two pictures are registered exactly.

**Hyp.5** for the time being, we consider there are no shadows.

- Hypothesis 1 approximatively holds as most city surfaces are rough (concrete,asphalt,...). Cases where this hypothesis would not hold are cases like wet tile or glass roofs which have a strong specular component.
- Hypothesis 2 is natural as there only is a punctual source of light at infinity (the sunlight). It can create ambient light due to diffusion of the sunlight in the atmosphere and reflexions on the ground.
- Hypothesis 3 relies on the geometrical structure of urban scenes. It is more difficult to describe, as different regions of the world might have different kinds of constructions. Nevertheless, most buildings have a common characteristic: our claim is that they are generally piecewise developable. Hemispherical roofs are very rare. Figure (6) comes from [16] where the authors create a dictionary of shapes corresponding to portions of European style buildings. They all satisfy this hypothesis.
- Hypothesis 4 is a strong hypothesis. In practice two airborne or satellite images are seldomly taken exactly from the same position. This introduces parallax errors as depicted in Figure (5). Reducing these issues requires non-rigid registration techniques. They are still under developpement, with interesting perspectives (see for instance [9, 15, 21]). In our experiments we only applied rigid registration, which explains some false positives.
- To simplify the discussion, we will deal with shadows later on. This means that the directional light lies everywhere in the scene.

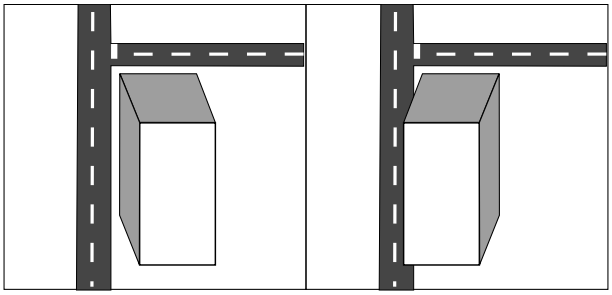

Figure 5: Illustration of parallax errors : two identical scenes are rendered with different geometries.

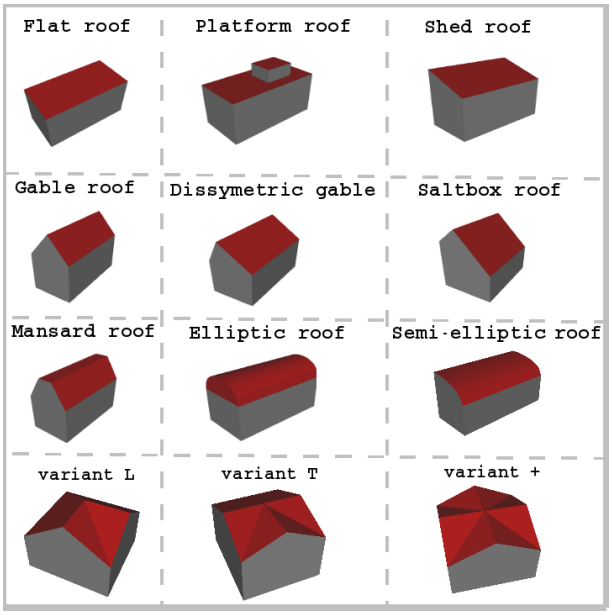


Figure 6: Dictionnary of roofs used in [16] to model european style cities. All of them are made of portions of developable surfaces. By courtesy of F. Lafarge.

## 4.2 A contrast equalization algorithm

Under the previous hypotheses we saw that the level lines of urban area images should be "almost" invariant to illumination changes. We propose a contrast enhancement and a change detection procedure that take advantage of this result. Let $u_1$ and $u_2$ be two exactly

registered images taken under different lighting conditions $L_1$ and $L_2$ at times $t_1$ and $t_2$. Let $S_1$ be the 3-D scene at time $t_1$. Under these assumptions we can write:

$$\left\{ \begin{array}{rcl} u_1 & = & u_{S_1,L_1} \\ u_2 & = & u_{S_1,L_2} + c_{1,2} \end{array} \right. \tag{4}$$

where $c_{1,2}$ denotes the changes from image $u_1$ to image $u_2$. In this equation $u_{S_1,L_2}$ and $c_{1,2}$ are unknown. To retrieve them, we need to introduce priors. From the previous discussion, it is natural to consider that $u_{S_1,L_2}$ should belong to the space of images which have the same level lines as $u_1$. We denote this space $\chi_{u_1}$. We can also devise a prior on the changes $J(c)$. In most applications, the changes are sparse. In this paper, as the $L^1$-norm is well known to favor sparse structures, we simply set $J(c) = ||c||_1$. To retrieve $c_{1,2}$ we can thus solve the following problem:

$$\inf_{u \in \chi_{u_1}} (||u_2 - u||_1) \tag{5}$$

and set $c_{1,2} = u_2 - \bar{u}$ where $\bar{u}$ is the solution of (5). Problem (5) can be reformulated as follows : "find the image $u$ closest to $u_2$ which has the same level lines as $u_1$". It is therefore a problem of contrast equalization. To solve (5) we need to discretize $\chi_{u_1}$. We propose the following simple strategy:

1. Set $u_Q = \lfloor \frac{u_1}{\Delta} \rfloor \Delta$ (uniform quantization).
2. For each level $k\Delta$ ($k \in \mathbb{Z}$), separate the connected components $\Omega_{k,j}$ of the set $\Omega_k = \{x \in \mathbb{R}^n, u_Q(x) = k\Delta\}$. In the experiments, we use the 8-neighbourood to define the notion of connected component.

We define $\chi_{u_1}$ as the set of images that are constant on each set $\Omega_{k,j}$. With this definition, the solution of (5) is in closed form:

$$\bar{u}|_{\Omega_{k,j}} = \text{median}(u_2|_{\Omega_{k,j}}) \tag{6}$$

This kind of algorithm has already been used and analyzed with a different motivation in [4]. This is a very fast algorithm (less than 0.4 second for a $1000 \times 1000$ image on an Intel Xeon CPU @ 1.86GHz). Let us finally point out that this algorithm is non symmetric. We can solve the following problem:

$$\inf_{u \in \chi_{u_2}} (||u_1 - u||_1) \tag{7}$$

and retrieve another change image $c_{2,1} = u_1 - \bar{u}$. In general we obtain $c_{1,2} \neq c_{2,1}$. This is a useful feature which allows to determine which scene contains a given detected object (see Fig. 8).

# 5 Results

In this section, we compare our approach with two classical algorithms, namely the monotone projection [25] and the change detection using the Fast Level Set Transform (FLST) [1, 27]. We choose these algorithms as both are asymmetric. The first one is a fundamental tool of image processing while the second one is based on similar principles as ours. We briefly describe them, then compare them on synthetic and real data.

## 5.1 Description of alternative approaches

### 5.1.1 Monotone projection

The monotone projection is described in [25]. It is similar to a global contrast equalization. We choose it for comparison as it is more general than a linear contrast equalization [30, 40]. As in paragraph (4.2), we suppose that we have two images that can be written as:

$$\begin{cases} u_1 = u_{S_1,L_1} \\ u_2 = u_{S_1,L_2} + c_{1,2} \end{cases} \tag{8}$$

The principle of the monotone projection is to consider that two images of the same scene taken under different illuminations differ only by a global monotonic contrast change. This means that $u_{S_1,L_2} = g \circ u_{S_1,L_1}$ where $g : \mathbb{R} \to \mathbb{R}$ is a non decreasing function. To retrieve the changes we can therefore find the function $\overline{g}$ which minimizes the following energy:

$$\overline{g} = \underset{g \text{ non decreasing}}{\arg\min} \left( ||g \circ u_1 - u_2||_2^2 \right) \tag{9}$$

Finally, we set $c_{1,2} = \overline{g} \circ u_1 - u_2$. Problem (9) can be solved in $O(n)$ operations where $n$ is the pixels number [25].

### 5.1.2 Comparison of the level set trees

Ballester *et al.* [1] and Monasse *et al.* [27] propose a contrast invariant algorithm for change detection. This algorithm is close to ours since it makes a large use of the level lines.

The algorithm principle is the following: first, each image is decomposed into a tree of "shapes" (the connected components of the image level sets). Figure (7) shows the FLST of two different functions. The two trees are then compared. A shape in the tree of $u_1$ will be said to match in the tree of $u_2$ if there exists a shape in this tree that has approximatively the same moments (position, area, ...). In Figure (7), the non-matching shapes would be the shapes labeled 2. The change images $c_{1,2}$ and $c_{2,1}$ are then recomposed from the non-matching shapes. We refer the reader to [27, 1] for more details about this method.

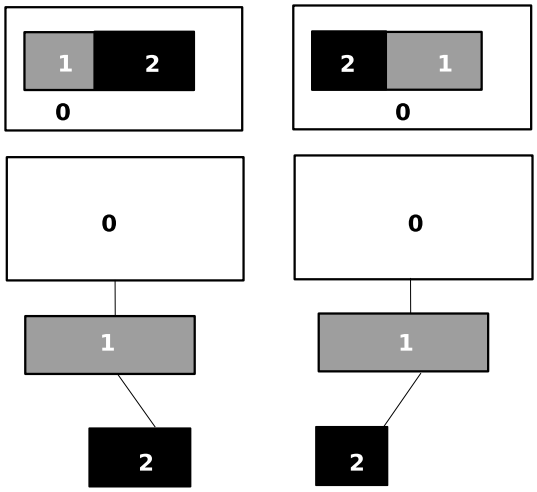


Figure 7: Top: images of a "triangle" shaped roof under different illuminations. Bottom: FLST of each image.

## 5.2 Synthetic images

To outline the results presented in this paper, we devised a simple 3-D scene generator which allows one to visualize simple instances of cities under different lighting conditions. The top images in Figure (8) show two images of "urban" areas. In this example, some buildings appeared or disappeared, the shape of some elements changed and some buildings moved.

In this toy example, the scene does not belong to $\Xi$ (one of the buildings is a dome), but all the other hypotheses of our model are satisfied. It clearly shows the assets of our method:

- The output of the monotone projection algorithm is clearly not satisfactory. A global monotonic contrast change cannot reproduce local grey value inversions. This explains the many false positives on the triangle rooftops.
- The reason of the failure of the FLST is more subtle. First, in our experiments we compare shapes only using their barycenter and their area. Such a measure is too naive to give satisfactory results. In [27, 1], the authors suggest to use higher order moments. However, this makes parameter evaluation more difficult.

  Moreover, even with a good measure of comparison the method should fail because the level set transform is not illumination invariant. For example, Figure (7) shows an image of a triangle shaped roof under two different illuminations. We can see that the level set trees are different. When comparing the two images, the shapes labeled "2" cannot match. Those shapes will thus be evaluated as changed by the algorithm.

- The output of our algorithm is very satisfactory. It fails on the dome (Gaussian curvature is not null), for a few level lines and for the top cylinder-shaped building. This is expected since the dome is not developable and that the level lines are only "almost" invariant. Between the two shots, the top cylinder-shaped building moves along its axis, only the non-overlapping parts of it are detected as changed.

## 5.3 Natural images

Let us now turn to real images. Our assumptions on the scene surface are only met at large scales. The roof tiles, for instance, can seldom be considered as developable, whereas the whole roof can. To apply the previous algorithm, we thus begin by a fast cartoon+texture decomposition algorithm [39] and only work on the cartoon parts. In the following experiments we used the Rudin-Osher-Fatemi model [31]. Furthermore we have not considered shadows in our model. Shadowed regions are only lightened by ambient light. Their intensity can generally be considered as a tenth of the regions lightened by directed light [38]. We thus remove the changes due to shadows by not considering the low intensity changes. Note that there exist more advanced techniques to remove shadows [13].

We provide comparisons on two Quickbird images. All the methods depend on a thresholding parameter. We thus provide ROC curves to compare the performances of the algorithms when the thresholds vary. Note that we defined the ground truth by hand for the two sets of images:

- **Airport of Abidjan**. On that image, the changes are quite easy to detect. All algorithms perform well.

  Compared with a classical approach (*i.e.* global contrast equalization followed by a per-pixel difference, bottom left), our algorithm yields satisfactory results, with few false negatives and much fewer false positives in very short times (3 seconds for the presented image). Our implementation of the FLST doesn't yield satisfying results compared with the other approaches. This might be due to the fact that we compare shapes only using their barycenter and area. As mentioned before, results can be imporoved by using higher order moments, but this increases the complexity of the parameter evaluation. This problem is important as the shapes matching algorithm takes around 30 seconds.

  The ROC curves (see Fig.11) show that our algorithm clearly outperforms the other approaches. For this pair of images, we can obtain 85% true positives with only 5% false positives whereas the other algorithms generate more than 20% false positives to achieve the same rate of true positives.

  The main reason for failure of our algorithm is the problem of registration: some painted lines on the taxiway are not exactly registered and some buildings edges do not coincide. Some false positives occur due to seasonal changes in the vegetation surrounding the taxiway.

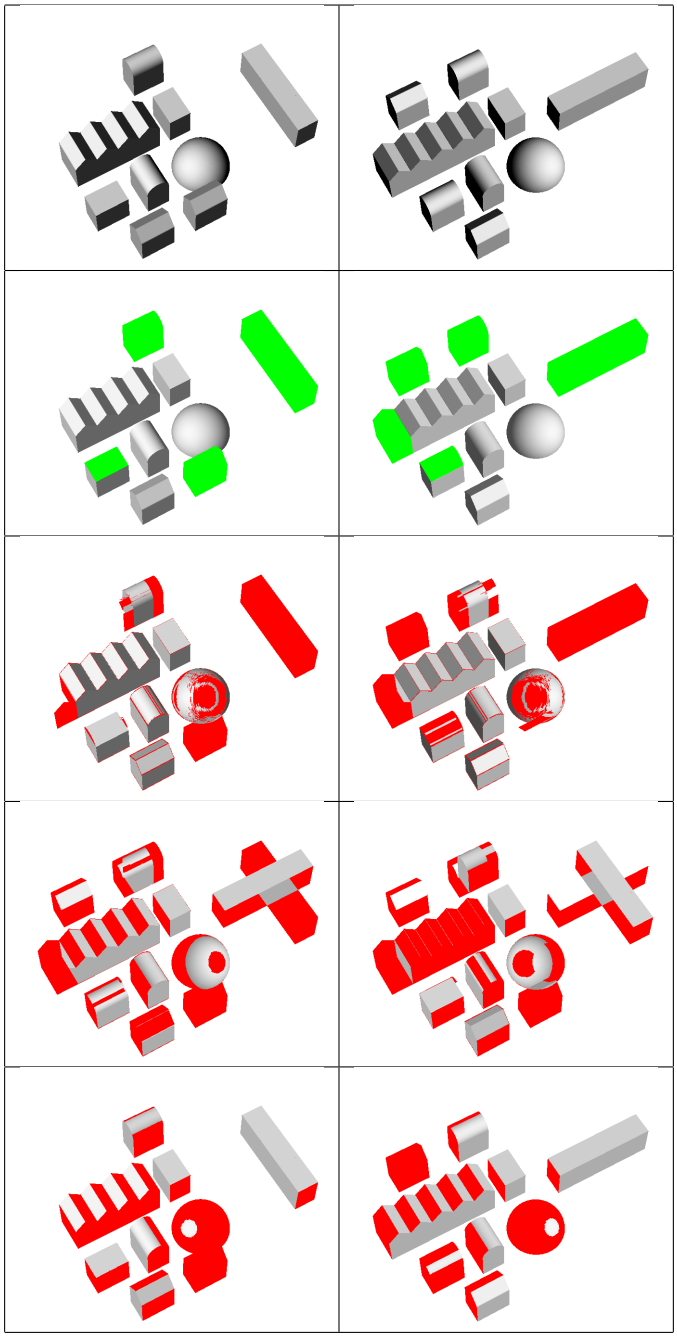

Figure 8: Toy example. First row: two images under different lighting conditions with some changes. Second row: the changes are depicted in green (ground truth). Third row: change detection using our algorithm. Fourth row: change detection using a least square contrast equalization. Fifth row: change detection using the FLST.

- **City of Beijing**. This pair of pictures is more challenging than the previous one. Huge modifications of the landscape occured between the two shots. Only a coarse ground truth can be obtained. Our algorithm still gives satisfactory results: very few false positives are obtained and a large part of the changes are detected. With a correctly chosen, we obtain 75% true positives and only 25% false positives. The other methods yield many false positives and their output seems difficult to use (see ROC curves Fig.12)).

# Conclusion

In this work we characterized the scenes that produce images with illumination invariant level lines. Based on this result, we proposed a contrast equalization and change detection algorithm. This simple and fast algorithm gives good results. Designing more precise change detection algorithms would require further semantic interpretation of the scenes. We hope that our theoretical contribution and practical experiment will encourage other researchers to use the level lines in more complex frameworks.

# Acknowledgment

The authors greatfully acknowledge Omid Amini for his invaluable help in the proof of theorem (2). They thank Alexis Baudour, Xavier Descombes, Véronique Prinet and Josiane Zerubia for fruitful discussions and support during the elaboration of this paper. They would also like to thank the RSIU team at Liama laboratory, Beijing, for kindly providing the high resolution image pairs of Beijing and F. Lafarge for providing the building library (Figure (6)). The second author would like to thank the French Defense Agency (DGA) for partial funding of his PhD and for providing the Quickbird images of Abidjan.

The next sections contain all the proofs of the propositions and theorems stated in the paper.

# A Proof of theorem (1)

*Proof.* Let us first express the gradient of $u$ in terms of $(s, \alpha)$ and $(l, \gamma)$. Simple geometry leads to $N(\mathbf{x}) = \Psi(\nabla s(\mathbf{x})) = \frac{(-s_1(\mathbf{x}), -s_2(\mathbf{x}), 1)}{\sqrt{s_1^2(\mathbf{x}) + s_2^2(\mathbf{x}) + 1}}$, where $s_1$ and $s_1$ are the derivatives of $s$ along the two axes of the object plane. Let $\mathbf{x} = p^{-1}(x)$. Using the chain rule and equation (2), we get that:

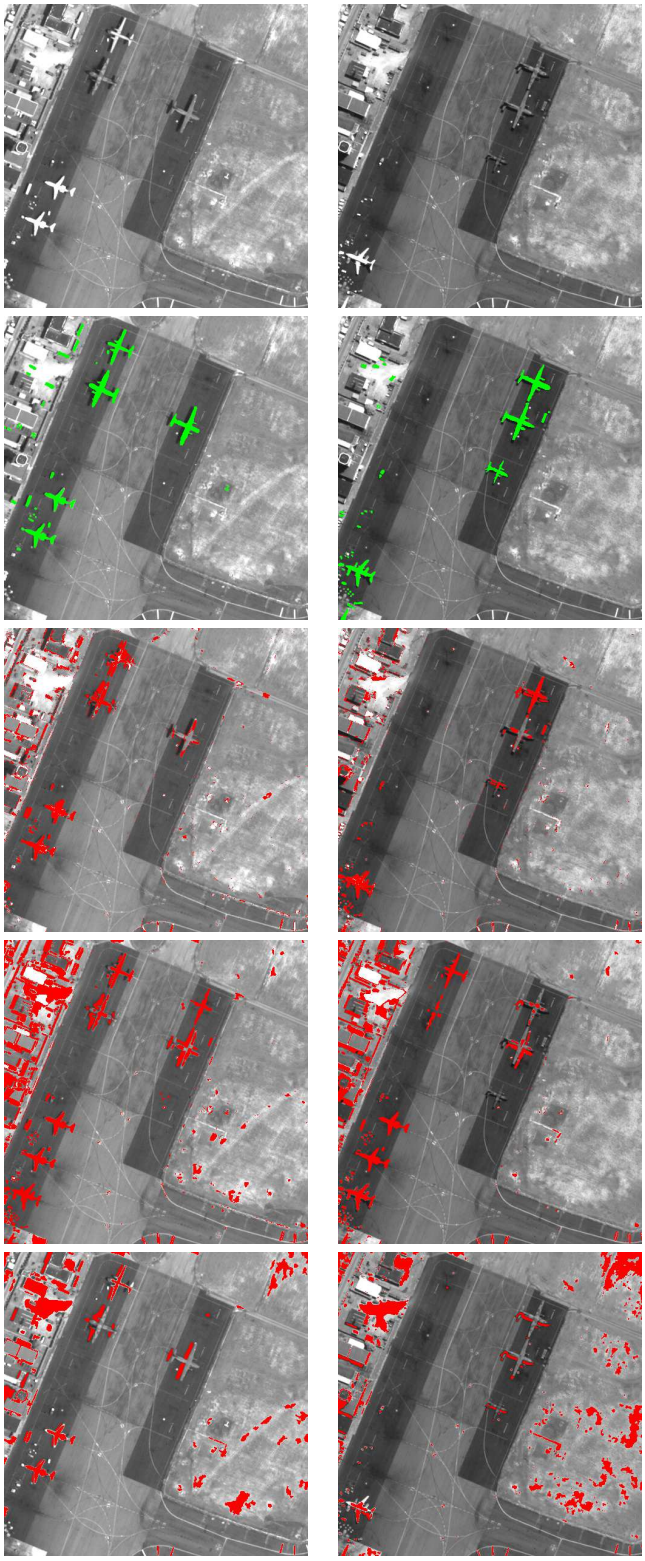



Figure 9: Quickbird images (61$cm$ resolution) of Abidjan airport. First row: Airport 04/02/2003 and 07/07/2003. Second row: ground truth (the changes are depicted in green). Third row: change detection using our algorithm. Fourth row: change detection using a least square contrast equalization. Fifth row: change detection using the FLST.

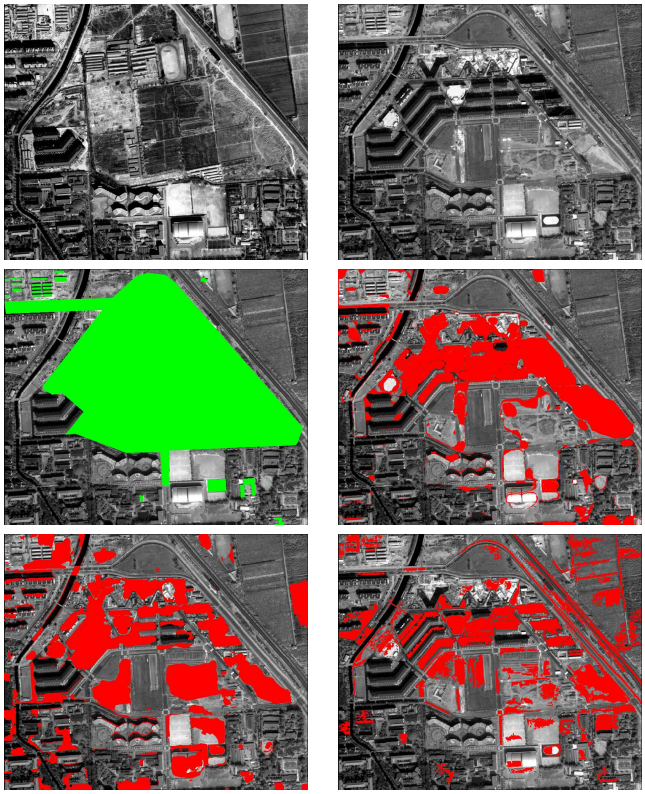

Figure 10: Quickbird images (61$cm$ resolution) of Beijing. First row: Beijing in 2001 (left) and 2003 (right). Second row - left: ground truth (the changes are depicted in green) - right: Change detection using our algorithm. Third row - left: change detection using a monotone projection - right: change detection using the FLST.

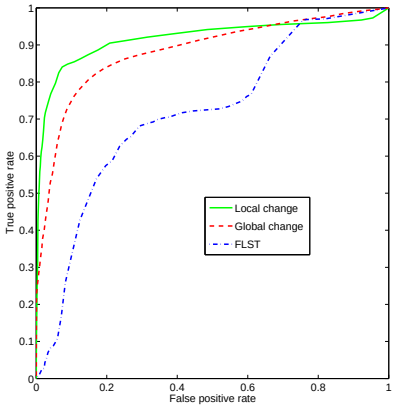


Figure 11: ROC curves for Abidjan airport.

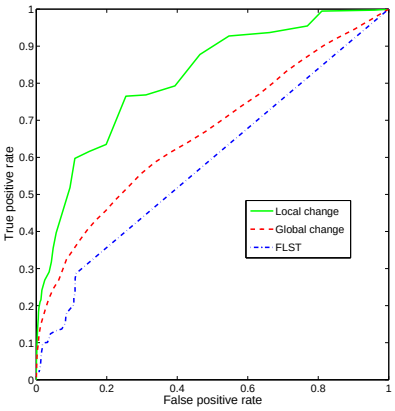


Figure 12: ROC curves for Beijing suburb.

$$\nabla u_{S,L}(x) = \left( \underbrace{l}_{\in \mathcal{M}_{1,3}} \cdot \left[ \underbrace{\Psi'(\nabla s(\mathbf{x}))}_{\in \mathcal{M}_{3,2}} \cdot \underbrace{\nabla^2 s(\mathbf{x})}_{\in \mathcal{M}_{2,2}} \underbrace{\alpha(\mathbf{x})}_{\in \mathbb{R}} + \underbrace{\Psi(\nabla s(\mathbf{x})}_{\in \mathcal{M}_{3,1}} \cdot \underbrace{\nabla \alpha(\mathbf{x})}_{\in \mathcal{M}_{1,2}} \right] + \underbrace{\gamma \nabla \alpha(\mathbf{x})}_{\in \mathcal{M}_{1,2}} \right) \cdot \underbrace{J(p^{-1})(x)}_{\in \mathcal{M}_{2,2}}$$

This can be rewritten as:

$$\nabla u_{S,L}(x) = (l \cdot A(\mathbf{x}) + \gamma \nabla \alpha(\mathbf{x})) \cdot J(p^{-1})(x) \tag{10}$$

with:

$$A(\mathbf{x}) = \left( \; [M_1, M_2] \cdot \begin{bmatrix} s_{11} & s_{12} \\ s_{12} & s_{22} \end{bmatrix} + N \cdot [\alpha_1, \alpha_2] \; \right)(\mathbf{x}) \tag{11}$$

$M_1(\mathbf{x}), M_2(\mathbf{x}) \in \mathcal{M}_{3,1}$ are the two columns of $\Psi'(\nabla s(\mathbf{x}))\alpha(\mathbf{x})$ and $N(\mathbf{x}) = \Psi(\nabla s(\mathbf{x}))$.
We gave the preliminaries to show *Prop. 1* $\Rightarrow$ *Prop. 2*. Let $S$ be a scene such that:

$$\forall (L_1, L_2) \in \mathscr{L} \times \mathscr{L}, \quad \forall x \in \Omega, \quad \nabla u_{S,L_1}(x) \mathbin{/\!\!/} \nabla u_{S,L_2}(x) \tag{12}$$

Let $D : \Omega \to \mathbb{S}^2$ denote the direction of invariance of $\nabla u_{S,L}$. On points $x$ where $\forall L \in \mathscr{L}, \;\; \nabla u_{S,L}(x) = 0$, $D$ might stick to any vector in $\mathbb{R}^2$.
As equation (12) must be true for all $([l_1, \gamma_1], [l_2, \gamma_2]) \in \mathscr{L} \times \mathscr{L}$, it needs to be true for $\gamma_1 = \gamma_2 = 0$. We thus neglect the term $\gamma[\alpha_X, \alpha_Y]$ in (10). Relation (12) can be rewritten:

$$\forall l \in \mathcal{L}, \; \forall x \in \Omega, \quad l \cdot A(\mathbf{x}) \cdot J(p^{-1})(x) \quad \mathbin{/\!\!/} \quad D(x) \tag{13}$$

As $p$ is a diffeomorphism, $J(p^{-1})(x)$ is a non-singular 2 by 2 matrix. Thus property (13) does not depend upon $J(p^{-1})$ and is true only if the matrix $A(\mathbf{x})$ has two parallel rows. This can be rewritten:

$$\begin{cases} (s_{11} M_1 + s_{12} M_2 + \alpha_1 N)(\mathbf{x}) &= a(\mathbf{x}) C(\mathbf{x}) \\ (s_{12} M_1 + s_{22} M_2 + \alpha_2 N)(\mathbf{x}) &= b(\mathbf{x}) C(\mathbf{x}) \end{cases} \tag{14}$$

where $(a, b) : \Omega \to \mathbb{R}^2$ and $C : \Omega \to \mathcal{M}_{3,1}$ are $C^0$ mappings. Some elementary (but fastidious) calculus leads to $\det([M_1, M_2, N](\mathbf{x})) > 0$, so that the vectors $M_1(\mathbf{x}), M_2(\mathbf{x}), N(\mathbf{x})$ form a basis of $\mathbb{R}^3$. System (14) thus implies that:

$$\begin{pmatrix} s_{11} \\ s_{12} \\ \alpha_1 \end{pmatrix}(\mathbf{x}) \mathbin{/\!\!/} \begin{pmatrix} s_{12} \\ s_{22} \\ \alpha_2 \end{pmatrix}(\mathbf{x}) \tag{15}$$

so that:

$$\begin{pmatrix} s_{11} \\ s_{12} \end{pmatrix}(\mathbf{x}) /\!\!/ \begin{pmatrix} s_{12} \\ s_{22} \end{pmatrix}(\mathbf{x}) /\!\!/ \begin{pmatrix} \alpha_1 \\ \alpha_2 \end{pmatrix}(\mathbf{x}) \tag{16}$$

Finally equation (16) leads to $\forall \mathbf{x} \in \mathbf{\Omega},\ \det(\nabla^2 s(\mathbf{x})) = 0$ which means that $s$ is developable. It is easy to check that the eigenvector of $\nabla^2 s(\mathbf{x})$ is $\begin{pmatrix} s_{12} \\ s_{22} \end{pmatrix}(\mathbf{x})$. This eigenvector is in the direction orthogonal to the generatrix of $s$ passing through point $\mathbf{x}$. Equation (16) thus indicates that $\alpha(\mathbf{x})$ varies in the direction orthogonal to this generatrix. For points such that $\nabla^2 s(\mathbf{x}) = 0$, no condition is imposed on $\alpha(\mathbf{x})$.

Now let us prove *Prop. 2 $\Rightarrow$ Prop. 1.* Let $S = (s, \alpha) \in \Theta$. This implies that $\forall \mathbf{x} \in \mathbf{\Omega},\ \det(\nabla^2 s(\mathbf{x})) = 0$. So that there exists $(c_1, c_2, a, b) : \mathbf{\Omega} \to \mathbb{R}^4$ such that:

$$\begin{bmatrix} s_{11} & s_{12} \\ s_{12} & s_{22} \end{bmatrix} = \begin{bmatrix} c_1 a & c_2 a \\ c_1 b & c_2 b \end{bmatrix} \tag{17}$$

with $c_1 b = c_2 a$. Moreover as the gradient varies orthogonally to the generatrices, there exists $c_3$ such that:

$$[\alpha_1, \alpha_2] = c_3 [a, b] \tag{18}$$

Using (17) and (18), the matrix $A$ (11) rewrites:

$$A = [aC, bC] \tag{19}$$

with $C = M_1 c_1 + M_2 c_2 + N c_3$. So that (10) simplifies to:

$$\nabla u_{S,L}(x) = ((\langle l, C \rangle + \gamma c_3)[a, b])(\mathbf{x}) \cdot J(p^{-1})(x) \tag{20}$$

and thus $\nabla u_{S,L}(x) /\!\!/ [a, b](\mathbf{x}) \cdot J(p^{-1})(x)$ for all $L \in \mathscr{L}$.

□

# B Proof of theorem (2)

In the following we prove theorem (2). In order to do so, we first need some preliminary lemmas.

**Lemma 1.** *Let $C : \Omega \to \mathbb{R}^4_*$ be a mapping (no regularity assumption is made).*
*Let $L \in \mathscr{L}$, $L^\perp$ denotes the hyperplane orthogonal to $L$.*
*Let $\omega_L = \mathrm{int}(\{x \in \Omega, C(x) \in L^\perp\})$.*
*For almost every $L \in \mathscr{L}$ (w.r.t. the Lebesgue measure of $\mathbb{R}^4$) $\omega_L = \emptyset$.*

*Proof.* Let us denote $Y = \{L \in \mathscr{L}, \omega_L \neq \emptyset\}$. Let $\Omega_{\mathbb{Q}} = \{\mathbb{Q}^2 \cap \Omega\}$. Since $\Omega_{\mathbb{Q}} \subset \mathbb{Q}^2$, $\Omega_{\mathbb{Q}}$ is a countable set.

Let $a_i \in \Omega_{\mathbb{Q}}$ and $Y_i = \{L \in \mathscr{L}, a_i \in \omega_L\}$. $Y_i$ is a subset of a hyperplane of $\mathbb{R}^4$. If it were not the case, there would exist four elements of $Y_i$, $L_1, L_2, L_3, L_4$ that would form a basis of $\mathbb{R}^4$. As $C(a_i) \perp L_j \ \ \forall j \in \{1,2,3,4\}$, it would mean that $C(a_i) = 0$ which contradicts $C(a_i) \in \mathbb{R}^4_*$.

Thus $\mu_{\mathbb{R}^4}(Y_i) = 0$ and $\mu_{\mathbb{R}^4}(\bigcup_{a_i \in \Omega_{\mathbb{Q}}} Y_i) = 0$. Furthemore $\bigcup_{a_i \in \Omega_{\mathbb{Q}}} Y_i = Y$ (since each non empty open set $\omega_L$ contains an element of $\mathbb{Q}^2$). Therefore, $\mu_{\mathbb{R}^4}(Y) = 0$.

□

**Lemma 2.** *Let $\omega \in \Omega$ be an open set. Let $u_1$ and $u_2$ be two $C^1(\Omega)$ functions such that: $\forall x \in \Omega,\ \nabla u_1(x) /\!\!/ \nabla u_2(x)$, $\nabla u_1(x) \neq 0$ and $\nabla u_2(x) \neq 0$. Then $u_1$ and $u_2$ have the same level lines on $\omega$.*

*Proof.* As $\nabla u_1$ and $\nabla u_2$ are non zero on $\omega$, the implicit functions theorem states that level lines of $u_1$ and $u_2$ are $C^1$ curves. Moreover, the curves can be defined based only using their respective normal: $\frac{\nabla u_1}{|\nabla u_1|}$ and $\frac{\nabla u_2}{|\nabla u_2|}$ which are equal. □

**Lemma 3.** *Let $u_1$ and $u_2$ be two $C^1(\Omega)$ functions such that: $\forall x \in \Omega,\ \nabla u_1(x) /\!\!/ \nabla u_2(x)$. The following propositions are equivalent:*

- *Prop. 1: $u_1$ and $u_2$ do not have the same level lines.*
- *Prop. 2: there exists a non-empty open set $\omega \subset \Omega$ such that:*

$$\forall x \in \omega, \quad \begin{cases} \nabla u_1(x) = 0 \\ \nabla u_2(x) \neq 0 \end{cases} \tag{21}$$

$$\text{or } \forall x \in \omega, \quad \begin{cases} \nabla u_1(x) \neq 0 \\ \nabla u_2(x) = 0 \end{cases} \tag{22}$$

*Proof. Prop. 2 ⇒ Prop. 1* is straightforward:

Since $\nabla u_1 = 0$ on $\omega$, $u_1$ is constant on $\omega$ and is thus included in a level line of $u_1$, whereas $\nabla u_2 \neq 0$ implies that $\exists (x,y) \in \omega^2$ such that $u_2(x) \neq u_2(y)$. Therefore $\omega$ is not included in a level line of $u_2$.

We prove *Prop. 1 ⇒ Prop. 2* by contradiction. Let us assume that there exists two $C^1(\Omega)$ functions $u_1$ and $u_2$ such that:

$(H_1)\ \forall x \in \Omega,\ \nabla u_1(x) /\!\!/ \nabla u_2(x)$

$(H_2)$ there exists no open set $\omega$ such that :

$$\forall x \in \omega, \begin{cases} \nabla u_1(x) = 0 \\ \nabla u_2(x) \neq 0 \end{cases} \tag{23}$$

$$\text{or } \forall x \in \omega, \begin{cases} \nabla u_1(x) \neq 0 \\ \nabla u_2(x) = 0 \end{cases} \tag{24}$$

$(H_3)$ The level lines of $u_1$ are different from the level lines of $u_2$

Let

$$\Omega_{1,0} = \{x \in \Omega, \nabla u_1(x) = 0\}$$
$$\Omega_{2,0} = \{x \in \Omega, \nabla u_2(x) = 0\}$$

1. *First we note that* $\mathring{\Omega}_{1,0} = \mathring{\Omega}_{2,0}$.

   Indeed, let us suppose:

   $$\begin{cases} \mathring{\Omega}_{1,0} \ \subset \Omega_{2,0} \\ \mathring{\Omega}_{2,0} \ \subset \Omega_{1,0} \end{cases} \tag{25}$$

   $\mathring{\Omega}_{1,0}$ being an open set, we have $\mathring{\Omega}_{1,0} \subset \mathring{\Omega}_{2,0}$. Applying the same reasoning, we get $\mathring{\Omega}_{2,0} \subset \mathring{\Omega}_{1,0}$, and finally $\mathring{\Omega}_{1,0} = \mathring{\Omega}_{2,0}$.

   Let us now suppose that (25) is false:

   $$\mathring{\Omega}_{1,0} \ \not\subset \Omega_{2,0} \text{ or } \mathring{\Omega}_{2,0} \ \not\subset \Omega_{1,0} \tag{26}$$

   Therefore, up to an inversion of the indices, there exists $x \in \mathring{\Omega}_{1,0} \setminus \Omega_{2,0}$ ($\nabla u_1(x) = 0$ and $\nabla u_2(x) \neq 0$). Therefore, from continuity of $\nabla u_2$ there exists an open set $\omega_x \subseteq \mathring{\Omega}_{1,0}$ containing $x$ such that $\nabla u_2 \neq 0$ on $\omega_x$. Moreover $\omega_x \subseteq \mathring{\Omega}_1^0$ implies that $\nabla u_1(x) = 0$ on $\omega_x$. This contradicts $(H_2)$.

2. We denote $\tilde{\Omega}^+ = \Omega \ \setminus \ \overline{\mathring{\Omega}}_{1,0}$. *On* $\tilde{\Omega}^+$*, the level lines of* $u_1$ *are different from those of* $u_2$.

   Again we prove this by contradiction. We suppose that the level lines of $u_1$ are the same as the level lines of $u_2$ on $\tilde{\Omega}^+$. According to last paragraph, $\nabla u_1$ and $\nabla u_2$ are zero on $\mathring{\Omega}_{1,0} = \mathring{\Omega}_{2,0}$. This can be extended by continuity to $\overline{\mathring{\Omega}}_{1,0}$. Therefore $u_1$ and $u_2$ are both constant on each connected component $U_i$ of $\overline{\mathring{\Omega}}_{1,0}$. Every $U_i$ is thus a level line of $u_1$ and $u_2$ on $\overline{\mathring{\Omega}}_{1,0}$. Let us now consider a level line $A$ of $u_1$ in $\tilde{\Omega}^+$. We can consider two cases.

   - $\forall i$, $U_i \cap A = \emptyset$. In that case, $A$ is clearly a level line of $u_1$ in $\Omega$. Since the same reasoning can be applied for $u_2$, $A$ is also a level line of $u_2$ in $\Omega$.

- $\exists i,\ U_i \cap A \neq \emptyset$. Both $A$ and $U_i$ are connected sets, then $A \cup U_i$ is a connected set. $u_1$ being continous, we get that $u_1$ constant on $A \cup U_i$. Similarly, $u_2$ is constant on $A \cup U_i$.

Thus, the level lines of $u_1$ and $u_2$ are the same on $\Omega$ which contradicts our hypotheses.

3. Let $\omega_1 \subset \Omega$ be an open set such that $\nabla u_1 = 0$ on $\omega_1$. Necessarily $\omega_1 \subset \mathring{\tilde{\Omega}}_1$ and thus $\omega_1 \cap \tilde{\Omega}^+ = \emptyset$. So there exists no open set in $\tilde{\Omega}^+$ on which $\nabla u_1 = 0$. This result also holds with $u_2$. let $\Omega_1^+ = \{x, \nabla u_1(x) \neq 0\}$ (resp. $\Omega_2^+ = \{x, \nabla u_2(x) \neq 0\}$). $\Omega_1^+$ and $\Omega_2^+$ are dense open sets in $\tilde{\Omega}_+$. Therefore (according to Baire's Theorem), $\Omega_1^+ \cap \Omega_2^+$ is a dense open set in $\tilde{\Omega}^+$.

4. From lemma (2), we know that the level lines of $u_1$ and $u_2$ are the same on $\Omega_1^+ \cap \Omega_2^+$. The continuity of $u_1$ and $u_2$ ensures that they are also the same on $\overline{\Omega_1^+ \cap \Omega_2^+} = \tilde{\Omega}^+$. This contradicts the conclusion of 2).

□

We now have all the elements to prove theorem (2).

*Proof of theorem (2).* We assume that $S \in \Theta$. This implies (*cf* proof of theorem (1)) that $\nabla u_{S,L} = \langle L, C \rangle \cdot [a, b]$ with $C : \Omega \to \mathbb{R}^4_*$, and $[a, b] : \Omega \to \mathbb{R}^2$, $C^0(\Omega)$ mappings. This yields $\forall (L_1, L_2) \in \mathscr{L} \times \mathscr{L}$, $\forall x \in \Omega$, $\nabla u_{S,L_1}(x) \mathbin{/\!/} \nabla u_{S,L_2}(x)$.

Let $\Omega^+ = \{x \in \Omega, [a, b](x) \neq 0\}$. This set is open as $a$ and $b$ are $C^0(\Omega)$. Let

$$\omega_L = \text{int}(\{x \in \Omega^+, \nabla u_{S,L}(x) = 0\}) \tag{27}$$

This set is also characterized by:

$$\omega_L = \text{int}(\{x \in \Omega^+, C(x) \in L^\perp\}) \tag{28}$$

From lemma (1), we get that for almost every $L_1 \in \mathscr{L}$, $\omega_{L_1} = \emptyset$. This implies that for almost every $L_1 \in \mathscr{L}$, $\forall \omega$ open set of $\Omega^+$, $\exists x \in \omega$ such that $\nabla u_{S,L_1}(x) \neq 0$. From the continuity of $\nabla u_{S,L_1}$, we get that there exists an open set $\omega_x \subset \Omega^+$ that contains $x$ on which $\nabla u_{S,L_1} \neq 0$. Now, for almost every $L_2 \in \mathscr{L}$, $\omega_{L_2} = \emptyset$, so that there exists $x' \in \omega_x$ such that $\nabla u_2(x') \neq 0$.

Hence, for almost every $(L_1, L_2) \in \mathscr{L} \times \mathscr{L}$, $\forall \omega \subseteq \Omega^+,\ \exists x' \in \omega$ such that :

$$\begin{cases} \nabla u_1(x') \neq 0 \\ \nabla u_2(x') \neq 0 \end{cases}$$

Furthermore, $\forall x \in \Omega \setminus \Omega^+$, $\nabla u_1(x) = \nabla u_2(x) = 0$.

Then note that the contraposition of lemma (3) is :

$$u_1 \text{ and } u_2 \text{ have the same level lines } \Leftrightarrow \tag{29}$$

$$\forall \omega \text{ open set of } \Omega^+,\ \exists x \in \omega, \tag{30}$$

$$\begin{cases} \nabla u_1(x) \neq 0 \\ \nabla u_2(x) \neq 0 \end{cases} \text{ or } \begin{cases} \nabla u_1(x) = 0 \\ \nabla u_2(x) = 0 \end{cases} \tag{31}$$

Thus we deduce that for almost every $(L_1, L_2) \in \mathscr{L} \times \mathscr{L}$, $u_{S,L_1}$ and $u_{S,L_2}$ have the same level lines. □

# C Other proofs

*Proof of corollary (1).* This is a direct consequence of theorem (1) and of the fact that two $C^1$ functions $u_1$ and $u_2$ have the same level lines only if $\forall x \in \Omega,\ \nabla u_1(x) /\!\!/ \nabla u_2(x)$. □

Let us rephrase proposition (1) more precisely :

**Proposition 2.** *Let $(\mathbf{x}_i, \mathbf{x}_j) \in \boldsymbol{\omega}_i \times \boldsymbol{\omega}_j$, where $(i,j) \in I^2$ and $i \neq j$, such that:*

- *there exists $y \in \overline{\kappa}_{\omega_i}(\mathbf{x}_i, L) \cap \overline{\kappa}_{\omega_j}(\mathbf{x}_j, L)$.*
- *for almost every $L'$ (w.r.t. the Lebesgue measure),*

$$\begin{cases} \overline{\kappa}_{\omega_i}(\mathbf{x}_i, L') = \overline{\kappa}_{\omega_i}(\mathbf{x}_i, L) \\ \overline{\kappa}_{\omega_j}(\mathbf{x}_j, L') = \overline{\kappa}_{\omega_j}(\mathbf{x}_j, L) \end{cases}$$

*Then:*

- *either we have:*

$$\lim_{\substack{\mathbf{x} \to \mathbf{y} \\ \mathbf{x} \in \boldsymbol{\omega}_i}} (N, \alpha)(\mathbf{x}) \neq \lim_{\substack{\mathbf{x} \to \mathbf{y} \\ \mathbf{x} \in \boldsymbol{\omega}_j}} (N, \alpha)(\mathbf{x}),$$

  *and for almost every $L$ (w.r.t. the Lebesgue measure), $u_{S,L}(x_i) \neq u_{S,L}(x_j)$.*

- *or we have:*

$$\lim_{\substack{\mathbf{x} \to \mathbf{y} \\ \mathbf{x} \in \boldsymbol{\omega}_i}} (N, \alpha)(\mathbf{x}) = \lim_{\substack{\mathbf{x} \to \mathbf{y} \\ \mathbf{x} \in \boldsymbol{\omega}_j}} (N, \alpha)(\mathbf{x}),$$

  *and for almost every $L$ (w.r.t. the Lebesgue measure), $u_{S,L}(x_i) = u_{S,L}(x_j)$.*

*Proof of Propositions (2).* Let $z \in \overline{\kappa}_{\omega_i}(\mathbf{x}_i, L) \cap \overline{\kappa}_{\omega_j}(\mathbf{x}_j, L)$ and $\mathbf{z} = p^{-1}(z)$. We have:

$$\forall x \in \kappa_{\omega_i}(\mathbf{x}_i, L),\ u(x_i) = u(x)$$

And in particular :

$$\begin{aligned} u(x_i) &= \lim_{\substack{x \to z \\ x \in \omega_i}} u(x) \\ u(x_i) &= \lim_{\substack{x \to z \\ x \in \omega_i}} \left( \left( \langle l, N \rangle + \gamma \right) \alpha \right) (\mathbf{x}) \end{aligned}$$

$z \in \overline{\kappa}_{\omega_i}(\mathbf{x}_i, L) \cap \overline{\kappa}_{\omega_i}(x_i, L)$ thus, $z \in \overline{\omega}_i \cap \overline{\omega}_j$. As $p$ is a diffeomorphism, $\mathbf{z} \in \overline{\boldsymbol{\omega}}_i \cap \overline{\boldsymbol{\omega}}_j$ and $\lim_{\substack{x \to z \\ x \in \omega_i}} \mathbf{x} = \mathbf{z}$. Therefore, according to our former hypotheses we can write:

$$u(x_i) = \langle l, \lim_{\substack{x \to z \\ x \in \omega_i}} (\alpha N)(\mathbf{x}) \rangle + \gamma \lim_{\substack{x \to z \\ x \in \omega_i}} \alpha(\mathbf{x}) \tag{32}$$

$$= \langle l, \lim_{\substack{\mathbf{x} \to \mathbf{z} \\ x \in \boldsymbol{\omega}_i}} (\alpha N)(\mathbf{x}) \rangle + \gamma \lim_{\substack{\mathbf{x} \to \mathbf{z} \\ \mathbf{x} \in \boldsymbol{\omega}_i}} \alpha(\mathbf{x}) \tag{33}$$

$$\tag{34}$$

Similarly, we have:

$$u(x_j) = \langle l, \lim_{\substack{\mathbf{x} \to \mathbf{z} \\ \mathbf{x} \in \boldsymbol{\omega}_j}} (\alpha N)(\mathbf{x}) \rangle + \gamma \lim_{\substack{\mathbf{x} \to \mathbf{z} \\ \mathbf{x} \in \boldsymbol{\omega}_j}} \alpha(\mathbf{x}) \tag{35}$$

Then $u(x_i) = u(x_j)$ if and only if:

$$\underbrace{\langle l, \lim_{\substack{\mathbf{x} \to \mathbf{z} \\ \mathbf{x} \in \boldsymbol{\omega}_i}} (\alpha N)(\mathbf{x}) - \lim_{\substack{\mathbf{x} \to \mathbf{z} \\ \mathbf{x} \in \boldsymbol{\omega}_j}} (\alpha N)(\mathbf{x}) \rangle}_{T_1} + \gamma \left( \lim_{\substack{\mathbf{x} \to \mathbf{z} \\ \mathbf{x} \in \boldsymbol{\omega}_i}} \alpha(\mathbf{x}) - \lim_{\substack{\mathbf{x} \to \mathbf{z} \\ \mathbf{x} \in \boldsymbol{\omega}_j}} \alpha(\mathbf{x}) \right) = 0 \tag{36}$$

We now consider two cases:

- if $\lim_{\substack{\mathbf{x} \to \mathbf{y} \\ \mathbf{x} \in \boldsymbol{\omega}_i}} (N, \alpha)(\mathbf{x}) \neq \lim_{\substack{\mathbf{x} \to \mathbf{y} \\ \mathbf{x} \in \boldsymbol{\omega}_j}} (N, \alpha)(\mathbf{x})$, then Eq. (36) is verified iff $L$ lies in a particular hyperplane of $\mathbb{R}^4$. Such plane is of zero Lebesgue measure.
- if $\lim_{\substack{\mathbf{x} \to \mathbf{y} \\ \mathbf{x} \in \boldsymbol{\omega}_i}} (N, \alpha)(\mathbf{x}) = \lim_{\substack{\mathbf{x} \to \mathbf{y} \\ \mathbf{x} \in \boldsymbol{\omega}_j}} (N, \alpha)(\mathbf{x})$, then we fall back to the smooth case, therefore : $u_{S,L}(x_i)$ and $u_{S,L}(x_i)$ form a single level line which is invariant for almost every illumination condition (w.r.t the Lebesgue measure).

□

# References

[1] C. Ballester, E. Cubero-Castan, M. Gonzalez, and J. Morel. Contrast invariant image intersection. *Advanced Mathematical Methods in Measurement and Instrumentation*, pages 41–55, 2000.

[2] F. Cao and P Bouthemy. A general principled method for image similarity validation. In *Proc. Int. Workshop on Adaptive Multimedia Retrieval*, volume 4398, pages 57–70, July 2006.

[3] V. Caselles, B. Coll, and J.M. Morel. Topographic Maps and Local Contrast Changes in Natural Images. *International Journal of Computer Vision*, 33, 1999.

[4] V. Caselles, B. Coll, and J.M. Morel. Geometry and Color in Natural Images. *JMIV*, 16:89–107, 2002.

[5] V. Caselles, J.L. Lisani, J.M. Morel, and G. Sapiro. Shape preserving local histogram modification. *IEEE Transactions on Image Processing*, 8:220–230, 1999.

[6] H.F. Chen, P.N. Belhumeur, and D.W. Jacobs. In Search of Illumination Invariants. *CVPR*, 2:254–261, 2000.

[7] H.F. Chen, P.N. Belhumeur, and D.W. Jacobs. In Search of Illumination Invariants. *submitted to IJCV*, 2008.

[8] F. Courteille, A. Crouzil, J.-D. Durou, and P. Gurdjos. Shape from shading for the digitization of curved documents. *Machine Vision and Applications*, 18(5):301–316, october 2007.

[9] M. Droske and M. Rumpf. A variational approach to non-rigid morphological registration. *SIAM Appl. Math.*, 64(2):668–687, 2004.

[10] A. Fournier, X. Descombes, and J. Zerubia. Mixing geometric and radiometric features for change classification. In *Proc. SPIE Symposium on Electronic Imaging*, 2008.

[11] F. Guichard and J.M. Morel. *Image Analysis and P.D.E.s.* to be published, 2001.

[12] B.K.P. Horn and M.J. Brooks. *Shape from shading.* MIT Press, 1989.

[13] R.B. Irvin and D.M. McKeown. Method for exploiting the relationship between buildings and their shadows in aerial imagery. *IEEE Trans. Syst. Man Cybern*, 19(12):1564–1575, 1989.

[14] K. Janisch. *Topology.* Springer, 1984.

[15] J. Kybic and M. Unser. Fast parametric elastic image registration. *IP*, 12(11):1427–1442, November 2003.

[16] F. Lafarge, X. Descombes, J. Zerubia, and M. Pierrot-Deseilligny. Building reconstruction from a single dem. In *CVPR*, june 2008.

[17] W. Li, X. Li, Y. Wu, and Z. Hu. A novel framework for urban change detection using vhr satellite images. In *International Conference on Pattern Recgnition*, pages 312–315, Washington, DC, USA, 2006. IAPR.

[18] R. Lillestrand. Techniques for change detection. *IEEE Trans. on Computers*, 21(7):654–659, 1972.

[19] C. Lin and R. Nevatia. Building detection and description from a single intensity image. *CVIU*, 72(2):101–121, 1998.

[20] J.L. Lisani and J.M. Morel. Detection of major changes in satellite images. In *ICIP*, pages 941–944, 2003.

[21] D.S. Liu, P. Gong, M. Kelly, and Q. Guo. Automatic registration of airborne images with complex local distortion. *PhEngRS*, 72(9):1049–1060, September 2006.

[22] D. Lu, P. Mausel, E. Brondiacutezio, and E. Moran. Change detection techniques. *International Journal of Remote Sensing*, 25(12):2365–2401, June 2004.

[23] D. J. Fleet M. J. Black and Y. Yacoob. Robustly estimating changes in image appearance. *Computer Vision and Image Understanding*, 78(1):8–31, 2000.

[24] D. Marr. *Vision: A Computational Investigation into the Human Representation and Processing of Visual Information*. W. H. Freeman and Company, NY, 1982.

[25] L. Moisan. *Modeling and Image Processing*. Lecture Notes of ENS Cachan edition, 2005.

[26] P. Monasse. Contrast invariant registration of images. In *ICASSP*, volume 6, pages 3221–3224, 1999.

[27] P. Monasse and F. Guichard. Fast computation of a contrast-invariant image representation. *IEEE Transactions on Image Processing*, 9:860–872, 2000.

[28] J. Mundy and A. Zisserman. *Geometric Invariance in Computer Vision*. MIT Press, Cambridge, 1992.

[29] B.T. Phong. Illumination for computer generated pictures. *Comm. ACM*, 18(6):311–317, June 1975.

[30] R.J. Radke, S. Andra, O. Al Kofahi, and B. Roysam. Image change detection algorithms: A systematic survey. *IEEE Transactions on Imagfe Processing*, 14(3):294–307, March 2005.

[31] L. Rudin, S. Osher, and E. Fatemi. Nonlinear Total Variation Based Noise Removal. *Physica D*, 60:259–268, 1992.

[32] M. Spivak. *A comprehensive Introduction to Differential Geometry*, volume 3. Publish or Perish, Inc., 1999.

[33] C.L. Tan, L. Zhang, Z. Zhang, and T. Xia. Restoring warped document images through 3d shape modeling. *IEEE Trans. on Pattern Analysis and Machine Intelligence*, 28(2):195–208, february 2006.

[34] F. Tang and V. Prinet. Computing invariants for structural change detection in urban areas. In *Urban Remote Sensing Joint Event, 2007*, pages 1–6, April 2007.

[35] J. Theiler and S. Perkins. Resampling approach for anomalous change detection. In *SPIE*, 2007.

[36] T. A. D. Toth and V. Metzler. Illumination-invariant change detection. *IEEE Southwest Symposium on Image Analysis and Interpretation*, 21(7):654–659, April 2000.

[37] T. Wada, H. Ukida, and T. Matsuyama. Shape from shading with interreflections under a proximal light source: distortion-free copying of an unfolded book. *IJCV*, 24(2):125–135, september 1997.

[38] S. Watanabe, K. Miyajima, and N. Mukawa. Detecting changes of buildings from aerial images using shadow and shading model. In *ICPR*, pages 1408–1412, 1998.

[39] P. Weiss, L. Blanc-Féraud, and G. Aubert. Efficient schemes for total variation minimization under constraints in image processing. RR 6260, INRIA, July 2007.

[40] R. Wiemker. An iterative spectral-spatial bayesian labeling approach for unsupervised robust change detection on remotely sensed multispectral imagery. In *CAIP*, pages 263–270, 1997.

Unité de recherche INRIA Sophia Antipolis
2004, route des Lucioles - BP 93 - 06902 Sophia Antipolis Cedex (France)

Unité de recherche INRIA Futurs : Parc Club Orsay Université - ZAC des Vignes
4, rue Jacques Monod - 91893 ORSAY Cedex (France)
Unité de recherche INRIA Lorraine : LORIA, Technopôle de Nancy-Brabois - Campus scientifique
615, rue du Jardin Botanique - BP 101 - 54602 Villers-lès-Nancy Cedex (France)
Unité de recherche INRIA Rennes : IRISA, Campus universitaire de Beaulieu - 35042 Rennes Cedex (France)
Unité de recherche INRIA Rhône-Alpes : 655, avenue de l'Europe - 38334 Montbonnot Saint-Ismier (France)
Unité de recherche INRIA Rocquencourt : Domaine de Voluceau - Rocquencourt - BP 105 - 78153 Le Chesnay Cedex (France)

Éditeur
INRIA - Domaine de Voluceau - Rocquencourt, BP 105 - 78153 Le Chesnay Cedex (France)
http://www.inria.fr
ISSN 0249-6399